

RESEARCH ARTICLE | FEBRUARY 21 2012

SiGe superlattice nanocrystal infrared and Raman spectra: A density functional theory study

Mudar A. Abdulsattar



J. Appl. Phys. 111, 044306 (2012)

<https://doi.org/10.1063/1.3686610>



Articles You May Be Interested In

Ab initio structural and vibrational properties of GaAs diamondoids and nanocrystals

AIP Advances (December 2014)

Structural and electrical studies of ultrathin layers with $\text{Si}_{0.7}\text{Ge}_{0.3}$ nanocrystals confined in a SiGe/SiO₂ superlattice

J. Appl. Phys. (May 2012)

Phase separation in SiGe nanocrystals embedded in SiO₂ matrix during high temperature annealing

J. Appl. Phys. (December 2008)

SiGe superlattice nanocrystal infrared and Raman spectra: A density functional theory study

Mudar A. Abdulsattar^{a)}

Ministry of Science and Technology, Baghdad, Iraq

(Received 21 September 2011; accepted 23 January 2012; published online 21 February 2012)

Infrared and Raman vibrational spectrum are calculated using *ab initio* density functional theory for SiGe superlattice nanocrystal of approximately 1.6 nm length. After obtaining the optimum positions of atoms via geometrical optimization using density functional theory, coupled perturbed Hartree-Fock equations are solved iteratively to obtain vibrational spectrum. Frequencies of vibrations are analyzed against intensities, reduced masses, and vibrational force constants. A scale factor of 0.81 is suggested to correct the frequencies of the present calculations that are obtained using STO-3 G basis functions. Results show that SiGe nanocrystals have complex and rich vibrational spectrum that can be generally divided into three regions. The highest reduced masses are in the first region where Si and Ge atoms are the main contributors to vibrations with a smaller number of vibrations attributed to hydrogen atoms. The highest intensity lines in SiGe superlattice nanocrystals are in the middle region where most of the modes of vibration can be excited. The third region is characterized by high force constants. The first region shows a redshift of the original Ge-Si bond vibration from the calculated bulk 418 cm^{-1} to the present nanocrystal 395 cm^{-1} . Hydrogen vibrations interferences are found in the same redshift region that might induce uncertainties in the experimentally measured redshift. Si-H and Ge-H vibrations are observed mainly in the second and third region and less frequently in the first region. These vibrations include modes of vibration such as symmetric, asymmetric, wagging, scissor, rocking, and twisting modes. © 2012 American Institute of Physics. [doi:10.1063/1.3686610]

I. INTRODUCTION

SiGe bulk material and nanocrystals gained spectacular attention during the past decades.^{1–7} This attention is due to expected many applications and superiority of its constituent ingredients i.e., Si and Ge in many semiconductor applications. The gap of bulk SiGe can be controlled by controlling the ratio of its ingredients in the range 0.67–1.11 eV. Although both Si and Ge are indirect bandgap semiconductors, superlattice of SiGe can have direct bandgap by controlling the thickness of each Si and Ge layers at the nanoscale.⁸ Nanocrystals of SiGe superlattice add another dimension to the control of gap value.²

In the present work we shall be concerned with the theoretical identification of infrared and Raman vibrational lines of SiGe superlattice nanocrystals and its comparison with experimental nanocrystals infrared and Raman spectrum lines. Since infrared and Raman spectra are one of major methods that can be used in determining materials characteristics,^{9,10} the present work results can be considered an important tool to identify SiGe superlattice nanocrystals.

II. THEORY

The present work is a continuation of previous work investigation of SiGe superlattice nanocrystals.² In the previous work we used density functional theory at the B3LYP level to calculate the electronic structure of SiGe superlattice nano-

crystals and compare the results with Si and Ge nanocrystals electronic structure. The calculated electronic structure is used in the present work to calculate vibrational spectrum intensities of SiGe superlattice nanocrystal. Coupled perturbed Hartree-Fock equations are solved iteratively to obtain vibrational frequencies.^{11,12} The solution starts with the Hessian matrix that evaluates the second derivative of the potential matrix with respect to Cartesian coordinates.^{11–13} This is a $3N \times 3N$ matrix where N is the number of atoms. Diagonalizing the above matrix we obtain eigenvectors and eigenvalues of vibrational modes. Using different techniques to separate rotational and translational motion modes of vibration we arrive at the $3N-6$ normal modes of vibration of this system of atoms.

The stoichiometry of the present nanocrystal is $\text{Si}_{32}\text{Ge}_{32}\text{H}_{84}$. The present SiGe nanocrystal represents a superlattice with the shortest period (1:1). The calculated frequencies using STO-3 G basis states must be corrected using a scale factor. Scale factors are usually introduced to account for the systematic errors that are produced in molecular orbital calculations.¹³ A previously suggested scale factor associated with density functional theory that incorporates STO-3 G basis is 0.9156.¹⁴ However we found this scale factor incorrectly reproducing the frequencies of the present nanocrystal. The presently suggested scale factor is 0.81. This scale factor matches excellently with experimental values as we shall see in the next sections. The cause of discrepancy of the old scale factor might be attributed to its derivation from first row small molecules and not for nanocrystals containing 2nd and 3rd row elements.

^{a)}Electronic mail: mudarahmed3@yahoo.com.

III. CALCULATIONS AND RESULTS

Program Gaussian03 (Ref. 15) is used for the present calculations to obtain discrete line frequencies of SiGe nanocrystal. With every calculated frequency there are other associated quantities that characterize this frequency. These quantities are line intensity, reduced mass, force constant, and normal coordinates of each atom in the nanocrystal. Unlike bulk materials, the number of frequencies in molecules or small nanocrystals is limited. The number of frequencies in the present nanocrystals is 438 frequencies, which correspond to the number of degrees of freedom in the nanocrystal.

In Fig. 1 intensities, force constants, and reduced masses of SiGe superlattice nanocrystal infrared and Raman spectra in the frequency range $10\text{--}470\text{ cm}^{-1}$ is shown. This figure is followed by a frequency gap of 40 cm^{-1} . Figure 2 shows the frequency range $510\text{--}934\text{ cm}^{-1}$. This figure is followed by a very wide frequency gap of 816 cm^{-1} . After this gap, Fig. 3 shows the frequency range $1750\text{--}2188\text{ cm}^{-1}$. Although these figures contain inner gaps that might be larger than that between the present figures, the division to the present three regions is made depending also on specific properties of

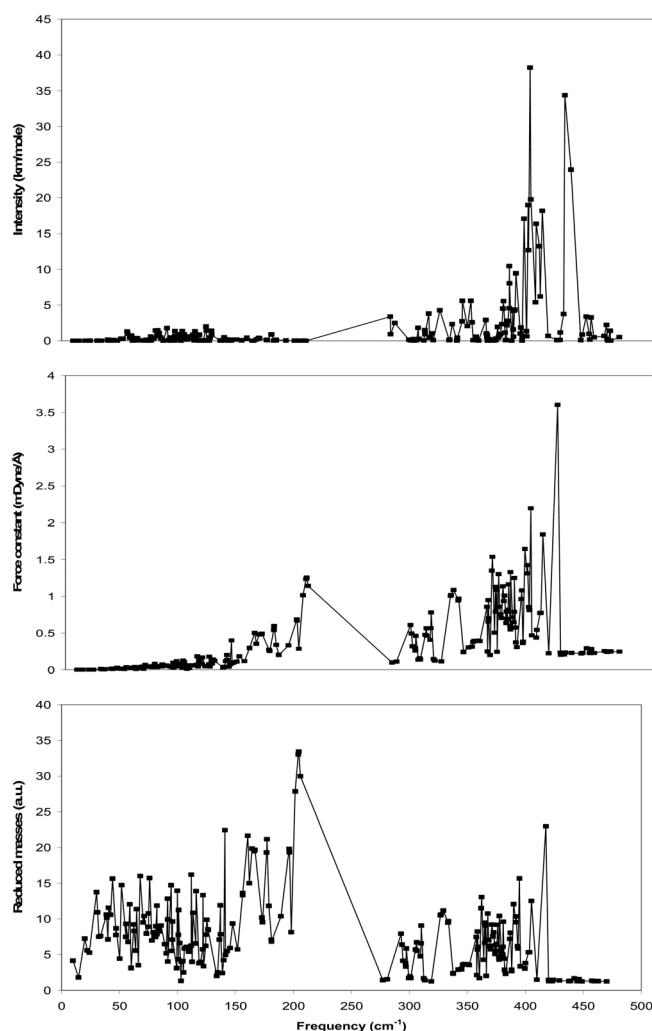


FIG. 1. Intensities, force constants, and reduced masses of SiGe superlattice nanocrystal infrared and Raman spectra in the frequency range $10\text{--}470\text{ cm}^{-1}$.

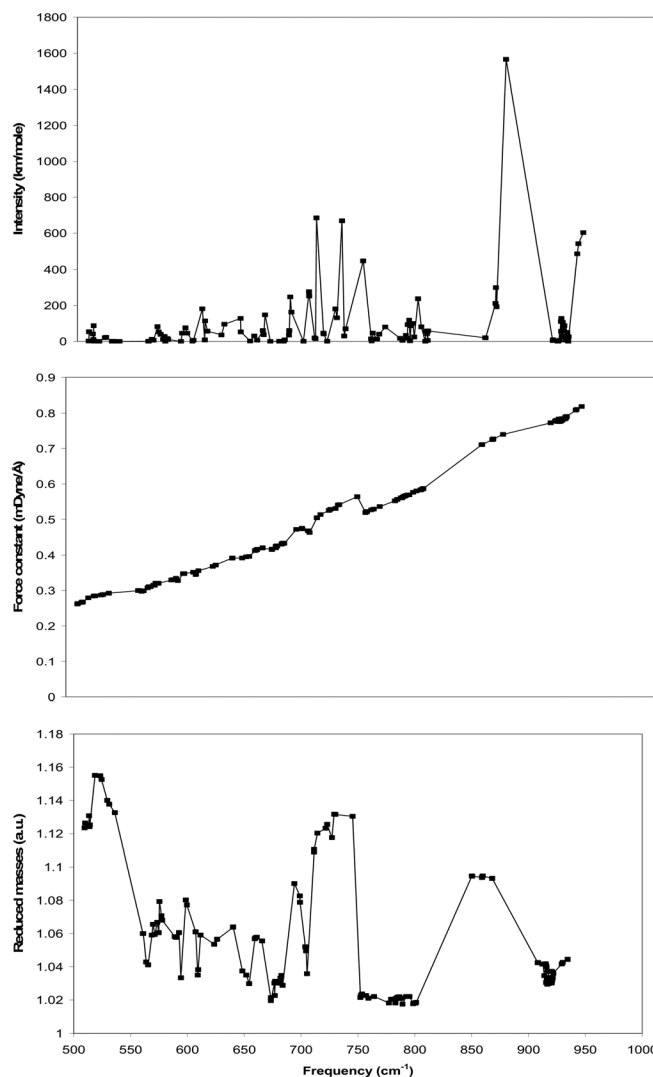


FIG. 2. Intensities, force constants, and reduced masses of SiGe superlattice nanocrystal infrared and Raman spectra in the frequency range $510\text{--}934\text{ cm}^{-1}$.

vibrations in these figures. As an example, Fig. 1 shows high reduced masses that are greater than that in Figs. 2 and 3. At the end of this figure, a small number of vibrations of small reduced masses are included in this figure because they show the same mode of vibrations similar of that inside Fig. 1. Figure 2, on the other hand, shows high intensity vibrations that is several times the intensities of other figures. Figure 3 in addition of being separated widely from Fig. 2, shows high force constant vibrations.

IV. DISCUSSION AND CONCLUSIONS

Unlike molecular vibrations, the selection rules of infrared and Raman transitions are very complex to trace in the present nanocrystal case. Simple symmetries are encountered in molecules because of limited number of atoms. The present more than 100 atoms nanocrystal contains more complex symmetries that usually contain contribution from the symmetries of wave functions of the allowed transitions of all the atoms in the present system of atoms. Collective oscillations of a large number of atoms that move in phase are usually responsible for the high transition rate lines.

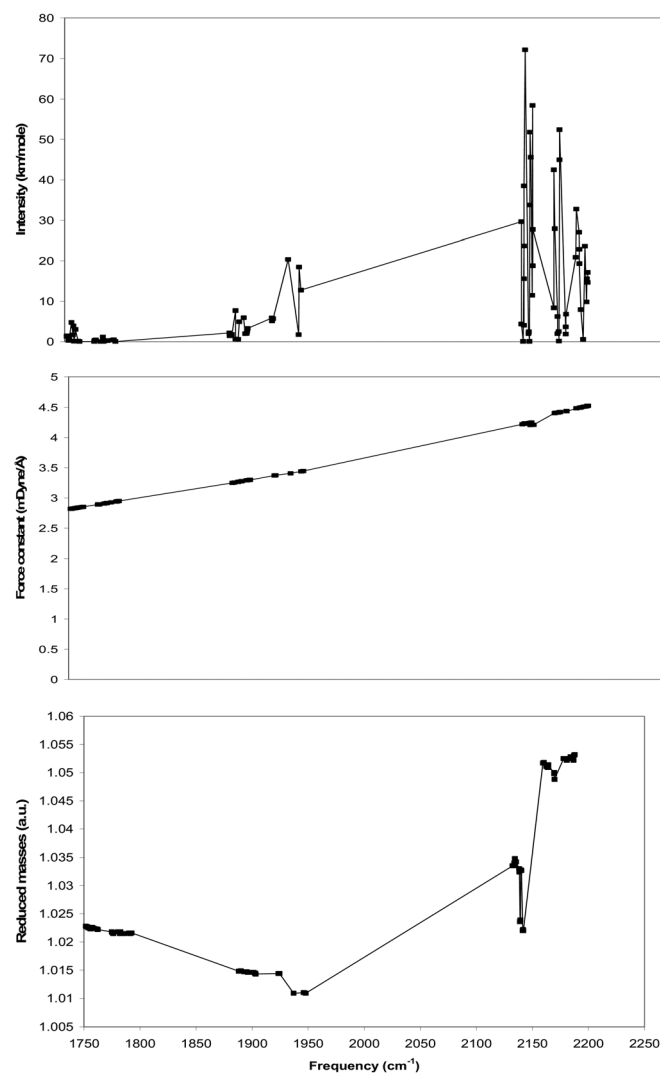


FIG. 3. Intensities, force constants, and reduced masses of SiGe superlattice nanocrystal infrared and Raman spectra in the frequency range 1750–2188 cm^{-1} .

It is well known that surfaces are symmetry breaking parts due to the breaking of translational symmetry encountered at the core of the nanocrystal. This broken symmetry adds additional difficulty to the already encountered by the high number of atoms. It is also well known that Hartree-Fock calculated forces is largely anharmonic, which throws away the remaining possible simplicity that might be gained if an approximate harmonic oscillator like analysis is applied. For these reasons we did not discuss these rules in the present manuscript and kept the final results in the present figures to manifest this difficulty.

The present nanocrystal is a hydrogenated SiGe superlattice nanocrystal that has the lowest periodicity (1:1), i.e., one layer of Si followed by other layer of Ge. As a result only Si-Ge vibrations are expected and no Si-Si or Ge-Ge can occur. The nanocrystal surface is passivated by hydrogen atoms so that hydrogen induced vibrations that are attached to both silicon (Si-H) or germanium (Ge-H) is expected.

Bulk silicon is identified by its near 520 cm^{-1} line.⁴ In the same way bulk SiGe crystals are identified by lines between that of silicon and germanium (germanium is slightly

greater than 300 cm^{-1} (Ref. 7)) depending on the composition of $\text{Si}_x\text{Ge}_{1-x}$ crystal. Since the present nanocrystal contains equal silicon and germanium atoms, the expected high intensity line should be very near to 415 cm^{-1} , which is the case in Fig. 1. Inspecting Fig. 1, we can note that the highest intensity line is lower in frequency than the expected bulk 415 cm^{-1} line. This fact reflects that surface reconstruction in nanocrystals changes bond length and strength so that only a small portion of the nanocrystal bonds remains in their ideal strength. The bulk vibrational frequency shift to a lower frequency in nanocrystals is known as the redshift.¹⁶

In order to identify different modes in the present nanocrystal we have to analyze the frequency results against reduced masses, force constants, and intensities. As we can see from Figs. 1, 2, and 3, the highest reduced masses are in the range of frequencies of Fig. 1. Two peaks of high intensity in Fig. 1 are in 395 and 424 cm^{-1} , which are the nearest to the expected bulk line at 415 cm^{-1} . However, the reduced masses of the two frequencies are 15.7 and 1.45 (a.u), respectively. This shows unambiguously that the first line is the red shifted bulk line. The second line is associated with hydrogen vibrations as we can see from the low reduced mass of the vibration. The vibration with the highest force constant in Fig. 1 is at 418 cm^{-1} . This line has a reduced mass of 23 (a.u.), which indicates that this is the original strong ideal bond of Si-Ge in the nanocrystal. The intensity of this vibration is relatively very low and is only 0.08 km/mole, which shows that a very small number of bonds is still in their original ideal strong condition.²

From the trend of reduced masses of Fig. 1 we can see two groups of data separated by a wide frequency gap at the range 206–277 cm^{-1} . The first group of data is associated with high reduced mass vibrations with one or two exceptions such as the point at 103 cm^{-1} with the reduced mass 1.3 (a.u.), which indicate a hydrogen induced vibration. Experimentally this peak is associated with transverse optical (TO) mode of GeH vibration at 116 cm^{-1} .¹⁷ The difference between the above two numbers shows that red shifting also applies to surface vibrations. Due to high force constant between hydrogen atoms and silicon or germanium atoms, low frequency vibrations move silicon or germanium atoms with their attached hydrogen atoms as one particle. This movement increases the reduced mass of such vibration as can be seen generally in this part of the spectrum in which reduced masses reaches 33 (a.u.).

The second group of data in Fig. 1, on the other hand, has a large number of low reduced mass vibrations that can be associated with several experimentally and theoretically calculated modes such as TO and rocking of GeH_2 (266, 333 cm^{-1}) and TO, wagging or rocking of GeH_3 (262, 429 cm^{-1}). The present mixing of vibrations in the redshift area with that of hydrogen induced vibrations complicates the identification of this redshift experimentally.

The second region in Fig. 2 (frequency range 510–934 cm^{-1}) is characterized by high intensity vibrations. Highest intensities of this region are 20 times larger than highest intensities in first and third regions. These high intensity vibrations indicate that excitations are induced by a high number of atoms that move collectively. The reduced masses of

this region are all indicating a nearly hydrogen induced vibrations. Experimental and previous calculations points to several modes of Si-H or Ge-H vibrations that match the present ranges of vibrations. These vibrations include GeH wagging (560 cm^{-1}), GeH_2 twisting, wagging, and scissor bending (555 , 567 , and 803 cm^{-1} respectively), GeH_3 symmetric deformations, degenerate deformation (699 , and 837 cm^{-1} respectively). All the Ge-H vibrations are taken from Table II of Ref. 17. Si-H vibrations exist in this region that include SiH bend (650 cm^{-1}), SiH_2 bend-scissor, wag, twist and rock, (900 , 850 , 820 , and 650 cm^{-1} , respectively), SiH_3 degenerate deformation, symmetric deformation, wag, rock and twist (900 , 850 , 630 , and 500 cm^{-1} respectively). All the Si-H vibrations are from Table I of Ref. 18.

Third region in Fig. 3 is in the range $1750\text{--}2188\text{ cm}^{-1}$. This region is very far from the second region, which is one of the reasons we separated it graphically from the second region. This region is characterized by high force constant and high variation in intensity at the last part of the spectrum. This region is divided to several parts. However, the first part ($1750\text{--}1950\text{ cm}^{-1}$) is attributed to the Ge-H vibrations. The second part ($2134\text{--}2188\text{ cm}^{-1}$) is attributed to Si-H vibrations. The first part can be matched with GeH stretching (1880 cm^{-1}), GeH_2 symmetric or asymmetric stretching (1995 , 2004 cm^{-1} , respectively), GeH_3 symmetric or asymmetric stretching (2041 , 2055 cm^{-1} respectively). The second part can be matched with, SiH_2 symmetric or asymmetric stretching (2100 cm^{-1}), SiH_3 symmetric or asymmetric stretching (2150 cm^{-1}). All Ge-H vibrations are from Table II of Ref. 17 while all Si-H vibrations are from Table I of Ref. 18. Redshift of some of the above mentioned lines can be seen from the above data.

Unlike single valued molecular vibration frequencies, range of adjacent frequencies is encountered in the present work. This is due to different second neighbors in nanocrystals atoms depending on the position of vibrating atom, which is a known phenomenon in molecular and solid state infrared calculations.^{9,10,17,18} Another reason is surface effect that undergoes a reconstruction that mostly weakens (with some exceptions) strength of vibrating bonds. Highest force constants are encountered in third region. These values are due to Si-H stretches. Ge-H stretches are smaller as can be seen in the first part of Fig. 3. Ge-H stretches force constants are generally stronger than Si-Ge vibration mode force constants with some exceptions as can be seen from force constant variation in all the figures.

As SiGe nanocrystals grow up in size, relative intensities will change in addition to the movement of the different lines of spectrum. The highest force constant line in region 1 will grow and increases in its intensity as the number of ideal bonds in the core of the nanocrystal increases.¹⁹ The relative intensity of the present highest intensity line in region 1 (395 cm^{-1}) will decrease and move toward the high force constant line (418 cm^{-1}). At the bulk crystal the two lines

coincides. The surface area of nanocrystals increases as the square of the dimension of the nanocrystal while the bulk volume increases as the third power of the dimension of the nanocrystal. As a result, the relative intensity of regions 2 and 3 (surface H vibrations) with respect to region 1 (mostly Si-Ge vibrations) will decrease. The number of the overall vibrations will increase and the gaps between vibration groups will decrease and might some times vanish. The spectrum will eventually turns into continues spectrum with varying intensity as we arrive at the bulk crystal.

As concluding remarks, the present results show that the use of an appropriate scale factor can greatly improves the matching between experimental and calculated frequencies of nanocrystals. The method can reproduce the nanocrystal redshift from bulk Si-Ge ideal vibration frequency peak. The method alarms experimentalist of the mixing of some Ge-H vibrations with red shifted Si-Ge original bulk frequency region that might complicates the separation of the right redshift frequency. Good match with experiment between different surface species such as Si-H and Ge-H can be obtained. The importance of nanocrystal surface inclusion in calculations can be seen from red shifted frequency identification and that two regions out of three are completely due to surface vibrations.

- ¹Y. Busby, M. De Seta, G. Capellini, F. Evangelisti, M. Ortolani, M. Virgilio, G. Grosso, G. Pizzi, P. Calvani, S. Lupi, M. Nardone, G. Nicotra, and C. Spinella, *Phys. Rev. B* **82**, 205317 (2010).
- ²M. A. Abdulsattar, *Superlattices Microstruct.* **50**, 377 (2011).
- ³S. F. Li, M. R. Bauer, J. Menéndez, and J. Kouvetakis, *Appl. Phys. Lett.* **84**, 876 (2004).
- ⁴M. Mermoux, A. Crisci, F. Baillet, V. Destefanis, D. Rouchon, A. M. Papon, and J. M. Hartmann, *J. Appl. Phys.* **107**, 013512 (2010).
- ⁵S. Nakashima, T. Mitani, M. Ninomiya, and K. Matsumoto, *J. Appl. Phys.* **99**, 053512 (2006).
- ⁶A. Picco, E. Bonera, E. Grilli, M. Guzzi, M. Giarola, G. Mariotto, D. Chrastina, and G. Isella, *Phys. Rev. B* **82**, 115317 (2010).
- ⁷R. Schorer, G. Abstreiter, H. Kibbel, and H. Presting, *Phys. Rev. B* **50**, 18211 (1994).
- ⁸M. Gell, *Phys. Rev. B* **40**, 1966 (1989).
- ⁹*Infrared and Raman Spectroscopy*, edited by B. Schrader (VCH Verlagsgesellschaft, Weinheim, 1995).
- ¹⁰D. W. Mayo, F. A. Miller, and R. W. Hannah, *Coarse Notes on the Interpretation of Infrared and Raman Spectra* (John Wiley & Sons, New York, 2003).
- ¹¹R. McWeeny, *Rev. Mod. Phys.* **32**, 335 (1960).
- ¹²R. McWeeny, *Phys. Rev.* **126**, 1028 (1962).
- ¹³J. B. Foresman and A. Frisch, *Exploring Chemistry with Electronic Structure Methods: A Guide to Using Gaussian*, 2nd ed. (Gaussian, Pittsburgh, 1996).
- ¹⁴S. Anand, O. Varnavski, J. A. Marsden, M. M. Haley, H. B. Schlegel, and T. Goodson, *J. Phys. Chem. A*, **110**, 1305 (2006).
- ¹⁵M. J. Frisch, G. W. Trucks, H. B. Schlegel *et al.*, GAUSSIAN 03, Revision B.01, Gaussian, Inc., Pittsburgh, PA, 2003.
- ¹⁶G. Faraci, S. Gibilisco, P. Russo, A. R. Pennisi, and S. LaRosa, *Phys. Rev. B* **73**, 033307 (2006).
- ¹⁷B. K. Ghosh and B. K. Agrawal, *Phys. Rev. B* **33**, 1250 (1986).
- ¹⁸G. Lucovsky, R. J. Nemanich, and J. C. Knights, *Phys. Rev. B* **19**, 2064 (1979).
- ¹⁹H. M. Abduljalil, M. A. Abdulsattar, and S. R. Al-Mansoury, *Micro Nano Lett.* **6**, 386 (2011).